Accepted to ApJ: January 4, 2008
Preprint typeset using LaTeX style emulateapj v. 10/09/06

arXiv:0801.2765v1 [astro-ph] 17 Jan 2008

QUIESCENT H_2 EMISSION FROM PRE-MAIN SEQUENCE STARS IN CHAMAELEON I

Jeffrey S. Bary[1], David A. Weintraub[2], Sonali J. Shukla[2], Jarron M. Leisenring[1] and Joel H. Kastner[3]
[1]Department of Astronomy, University of Virginia, P.O. Box 400325, Charlottesville, VA 22904-4325
[2]Department of Physics & Astronomy, Vanderbilt University, P.O. Box 1807 Station B, Nashville, TN 37235 and
[3]Carlson Center for Imaging Science, RIT, 54 Lomb Memorial Drive, Rochester, NY 14623

Accepted to ApJ: *January 4, 2008*

ABSTRACT

We report the discovery of quiescent emission from molecular hydrogen gas located in the circumstellar disks of six pre-main sequence stars, including two weak-line TTS, and one Herbig AeBe star, in the Chamaeleon I star forming region. For two of these stars, we also place upper limits on the $2 \rightarrow 1\ S(1)/1 \rightarrow 0\ S(1)$ line ratios of ~ 0.4 and 0.5. Of the 11 pre-main sequence sources now known to be sources of quiescent near-infrared hydrogen emission, four possess transitional disks, which suggests that detectable levels of H_2 emission and the presence of inner disk holes are correlated. These H_2 detections demonstrate that these inner holes are not completely devoid of gas, in agreement with the presence of observable accretion signatures for all four of these stars and the recent detections of [Ne II] emission from three of them. The overlap in [Ne II] and H_2 detections hints at a possible correlation between these two features and suggests a shared excitation mechanism of high energy photons. Our models, combined with the kinematic information from the H_2 lines, locate the bulk of the emitting gas at a few tens of AU from the stars. We also find a correlation between H_2 detections and those targets which possess the largest Hα equivalent widths, suggesting a link between accretion activity and quiescent H_2 emission. We conclude that quiescent H_2 emission from relatively hot gas within the disks of TTS is most likely related to on-going accretion activity, the production of UV photons and/or X-rays, and the evolutionary status of the dust grain populations in the inner disks.

Subject headings: infrared: stars — solar system: formation — stars: pre-main sequence — stars: individual (CS Cha, HD 97408, Sz 33, CV Cha, GM Aur, Glass I) — stars: protoplanetary disks — ISM: molecules

1. INTRODUCTION

The reservoirs of gas and dust found orbiting most sun-like stars with ages on the order of a million years — also known as T Tauri stars (TTS) — are now subjects of intense study, as they likely hold the secrets to the formation history of the solar system and other planetary systems. The evolution of the observable characteristics of these planet forming disks and the underlying phenomena responsible for their detectability may provide the necessary insight to further our understanding of planet forming processes and to determine the likelihood of the formation of planetary systems around sun-like stars.

The existence of circumstellar disks accompanying young low mass stars previously has been inferred by the presence of detectable emission from trace constituents of these disks (i.e., dust and gaseous molecules other than H_2). The earliest attempts to determine the fraction of stars that possess disks in young star forming clusters focused on their near-infrared continuum (Strom et al. 1989) and submillimeter continuum emission (Weintraub et al. 1989; Beckwith et al. 1990). Circumstellar disks possessing warm ($T \sim 1000$ K) micron-sized dust grains within ~ 1 AU of the pre-main sequence stars produce near-infrared emission in excess of that predicted for the stellar photosphere, while circumstellar disks possessing cold, micron-sized dust grains at radii of several tens of AU produce excess radiation at mid-infrared and submillimeter wavelengths. From surveys such as these, astronomers have determined the lifetime of warm dust grains in the inner disks to be 3-6 Myr (Lada et al. 2000; Haisch et al. 2000, 2001). Similarly, observations of cold ($T \sim$ 10-100 K) gas molecules (e.g., CO, HCN^+, etc) from the outer regions of the disks (Beckwith & Sargent 1993; Zuckerman et al. 1995) tend to support the disk lifetime estimates drawn from near-infrared surveys.

More recently, new disk fraction and lifetime surveys of TTS in nearby star forming regions have been conducted utilizing the Infrared Array Camera (IRAC) and Multiband Imaging Photometer (MIPS) aboard the *Spitzer Space Telescope*. These instruments are capable of detecting emission from dust grains ($T \sim$ 100-300 K) located at intermediate disk radii, a region of these disks to which the previous photometric surveys were insensitive. Cieza et al. (2007) took a census of 230 sources identified as weak-line TTS – weakly or non-accreting TTS possessing either a passive, optically thin disk or no circumstellar material – in the Lupus, Ophiuchus, and Perseus molecular clouds. They find a higher disk frequency for the sources located in the highest extinction regions of the clouds, suggesting that the wTTS at the edges of the formation regions are slightly older and more evolved. Although they find $\sim 20\%$ of these possess some circumstellar material, $\sim 50\%$ of what appear to be the youngest stars in the sample show no evidence of disks. These results, which are consistent with other *Spitzer* surveys of low mass star forming regions (Furlan et al. 2006; Geers et al. 2006; Kessler-Silacci et al. 2006; Padgett et al. 2006; Damjanov et al. 2007), lead them to conclude, based

Electronic address: jsb3r@virginia.edu,david.a.weintraub@vanderbilt.edu,sonali.j.shukla@vanderbilt.edu,jarron@virginia.edu,jhkpci@cis.rit.edu

on the existence of detectable emission from cool dust grains, that disk lifetimes are less than ten million years, which roughly agrees with the conclusions about disk lifetimes drawn from near-infrared surveys. Given the chaotic environment near these young stars and the phenomena (i.e., accretion, photoevaporation, stellar and disk winds, close encounters with other cluster members) that conspire to destroy these disks, the lifetimes measured from these surveys can be explained by disk dissipation models including all or some of these processes (Hollenbach et al. 2000).

Despite the growing consensus that disk lifetimes are only a few million years that has been drawn from several different techniques for studying circumstellar disks, astronomers must remain cautious when inferring the presence or absence of disks based upon the detectability of disk tracers (i.e., dust and CO emission) because the majority of the disk mass is composed of molecular hydrogen (H_2). As these disks evolve according to the core accretion model of planet formation, the small micron-sized dust grains accumulate into larger bodies, which will change the wavelength dependence of the dust emissivities and the collective surface area of dust grains emitting at wavelengths in the near-infrared. Since a planetesimal must reach a mass of $\simeq 10$ earth masses before it can gravitationally collect H_2 gas from the disk, the main component of the disk must persist, while planetesimals accrete into km-sized objects and disk tracers disappear, in order for gas giant planets to be the result of the core accretion scenario of planet formation. Therefore, in an accretionally-evolved system in which small dust grains have coagulated into larger planetesimals, an evolutionary stage should exist during which both the near-infrared and mid-infrared excesses will have diminished substantially while the massive gaseous component remains present.

In previous work, Weintraub et al. (2000), Bary et al. (2002), and Bary et al. (2003) searched a variety of TTS, predominantly wTTS, in the nearby Taurus-Auriga, ρ Ophiuchus, and TW Hya Association star forming regions for emission signatures from H_2 persisting in such accretionally evolved circumstellar disks. Using various high-resolution, near-infrared spectrometers, narrow line emission centered at the $v = 1 \rightarrow 0$ $S(1)$ transition rest wavelength of 2.1218 μm was detected from several TTS stars; some were known to possess circumstellar disks (TW Hya, GG TauA, and LkCa 15), and one was previously thought to be devoid of any circumstellar material (DoAr 21). The detection of quiescent emission from the disk of a wTTS with no other detectable disk tracers suggests that the gaseous component may indeed persist as the disk evolves. However, we estimate the mass of hot H_2 gas producing the observed features in these sources to be in the range 10^{-12}-10^{-10} $M_{\odot}$. For at least three of these four sources, a substantial reservoir of H_2 gas exists in their disks suggesting that the near-infrared H_2 emission feature, is itself only a tracer of the disk gas. In the time since these detections were made, several other authors searching for the same emission signature also have detected H_2 gas (Itoh et al. 2003; Takami et al. 2004; Ramsay Howat & Greaves 2007). In two of the three additional sources toward which H_2 was detected (LkHα 264 and ECHA J0843.3-7905), the emission lines were similarly centered at 2.1218 μm, with full-width at half of maximum (FWHM) only slightly larger than those reported for the previous four detections. In the case of DG Tau, Takami et al. (2004) reported the detection of an H_2 emission line blueshifted by 15 km s^{-1} and possessing a FWHM of ~ 35 km s^{-1}. The authors also show that the emitting gas is extended along the axis of a strong outflow previously observed from this source. Therefore, the emitting gas from this source is most likely associated with the outflowing gas distinguishing this detection from the others. In addition to these detections of rovibrational emission, Sheret et al. (2003), Bitner et al. (2007) and Martin-Zaïdi et al. (2007) have detected H_2 emission from the mid-infrared pure rotational transitions from the Herbig AeBe stars, AB Aur and HD 97048, with a similarly quiescent kinematic signature.

Here, we present five more detections of H_2 near-infrared emission from both classical and weak-line TTS, an infrared companion (IRC), and a detection from a Herbig AeBe star in the Chamaeleon I star forming region. In addition, we place an upper limit on emission from a second line of H_2 at 2.2477 μm for two of these sources. We review the possible stimulation mechanisms with respect to recent X-ray and UV irradiated disk models. We find that two of our past detections and one of the present detections possess transitional disks — disks with large inner disk holes devoid of emission from small warm dust grains. Two of these transitional disk sources also possess detectable emission from a mid-infrared [Ne II] emission line predicted to be a tracer of high energy photons and a signature of photoevaporation, a mechanism thought to be potentially responsible for the presence of the inner disk holes of the transitional disks. Kinematic information from the H_2 emission features suggest that the emitting gas extends to within a few AU of each source, demonstrating for the sources with inner disk holes that gas remains despite the lack of dust emission. We estimate the location of the regions within the disks where potential excitation photons deposit their energies and find agreement with the location of emitting gas determined from the velocity dispersion of the line. Finally, we relate the detection of quiescent H_2 emission to accretion activity and, possibly, the evolutionary status of the dust grain population.

2. OBSERVATIONS

We obtained high spectral resolution (R $\simeq$ 60,000) near-infrared spectra of thirteen TTS (Table 1) in the Chamaeleon I star forming region on 2003 January 7-18, UT, using the Phoenix spectrometer (Hinkle et al. 1998) in queue-mode on the Gemini South 8-m telescope atop Cerro Pachon in Chile. Phoenix utilizes a 256 × 1024 pixel section of a 1024 × 1024 pixel InSb Aladdin II detector. Most of our spectral observations were centered at 2.1218 μm and were made using a 14″ long, 0.″17 (2 pixel) wide slit, which result in nominal instrumental spatial and velocity resolutions of 0.″05 and ~ 5 km s^{-1}, respectively. For the observations of the two faintest sources, Sz 33 and CHX 20E, and follow-up observations centered at 2.2477 μm of CS Cha and HD 97048, we used the larger, 0.″34 (4 pixel) wide slit, resulting in a velocity resolution of ~ 6 km s^{-1}. Spectra centered at 2.1218 μm provided a spectral coverage from 2.1170 to 2.1262 μm, while those centered at 2.2477 μm covered 2.2426 to 2.2534 μm. The spectral region centered at

TABLE 1
CHA I SOURCE LIST

Source	Class [a]	Spectral Type [b]	Hα EW [c] (Å)	Log L_x [d] (ergs s^{-1})	A_v [e]
CS Cha	cTTS	K4	-13.3, -20, -65	30.0	0.85
HD 97408	AeBe	B9.5	-30.0	29.0	1.30
Sz 33	cTTS	M0	-9.5	28.9	1.45
Glass Ia	wTTS	K4	-4.0	30.1	1.92
Glass Ib	IRC	G5	-9.3	...	...
CV Cha	cTTS	G8	-60.5	30.1	1.67
Sz 41	wTTS	K0-K1	-2.7	30.2	1.17
LHα 332-17	cTTS	G2	-17.2	29.9	2.35
CHX 20E	wTTS	K4.5	0.0	29.4	0.31
Sz 30	wTTS	M0	-5.2	30.1	1.18
HD 97300	AeBe	B9	0	29.2	1.80
Ced110 IRS 2	wTTS	G2	>-1.2	30.7	3.39
WW Cha	cTTS	K5	-67.4	29.8	3.20

[a] Class of stars taken from Feigelson et al. (1993), Hamann & Persson (1992b), and Natta et al. (2000).[b] Spectral types taken from Feigelson & Kriss (1989), Gauvin & Strom (1992), Hamann & Persson (1992a), and Hamann & Persson (1992b).[c] Hα EWs from Appenzeller et al. (1983), Feigelson & Kriss (1989), Gauvin & Strom (1992), Walter (1992), and Luhman (2004).[d] Log L_x values taken from Feigelson et al. (1993).[e] Visual extinction values taken from Gauvin & Strom (1992).

the wavelength for the $v = 1 \rightarrow 0$ $S(1)$ H_2 transition includes three bright telluric OH lines, at 2.11766, 2.12325, and 2.12497 μm, while the spectra centered at the wavelength for the $v = 2 \rightarrow 1$ $S(1)$ transition contains two OH lines at 2.24599 and 2.25192 μm. These OH lines were used to provide an absolute wavelength calibration for each observation.

Using integration times of 900 s for our program stars (Table 1), we obtained signal-to-noise ratios (SNR) in the continua for all sources of ≥ 50, with the exception of the continuum for Sz 30, for which the SNR was lower. An integration time of 900 s also was used for the two observations of CS Cha and HD 97048, centered on the 2.2477 μm H_2 line. Our observing program included repeated 120 s observations of telluric calibration sources – HR 3685 (A2IV), HR 5571 (B2III), HR 4798 (B2V), HR 5231 (B2.5IV), and HR 1956 (B7IV) – possessing few, if any, photospheric features in this $K-$band portion of their spectra. Similar observations of HR 5231 and HR 5762 (A2IV) centered at 2.2477 μm used as telluric calibrators were made with shorter integrations times of 60 s and 40 s, respectively. Flat-field images were obtained using the Gemini Facility Calibration Unit Quartz Halogen lamp (Ramsay-Howat et al. 2000). Observations were made by nodding the telescope $5''.0$ along the slit, producing image pairs that were then subtracted to remove sky background and dark current. The spectra were extracted from $0''.25$ north to $0''.25$ south of the central row of pixels of the spectral beam, corresponding to the FWHM of the spectral beam. The target star spectra were then ratioed with one of the telluric calibration sources in order to remove telluric absorption features.

3. RESULTS

We have detected quiescent 2.1218 μm line emission from H_2 from four additional TTS (CS Cha, Sz 33, CV Cha, and Glass Ia), one IRC (Glass Ib, the secondary component to one of the TTS detections), and one Herbig AeBe star (HD 97048) in the Chamaeleon I star forming region. We define quiescent H_2 emission as emission at low velocities relative to and centered on the stellar rest velocity. These detections nearly double the total number of TTS known to have quiescent H_2 emission at this wavelength. Full spectra of both the detections and nondetections obtained with Phoenix are presented in Figure 1. For each source with detectable emission, with the exception of the binary system, Glass I, the emitting gas is determined to be within a single Gaussian-shaped spectral beam with a full-width of $\sim 1''$ placing the emission within ~ 80 AU of each of the sources (Cha I; D ~ 160 pc) . In the spectral images of Glass Ia and Ib, and the subsequent spectral extractions of Glass I, we find that the emission from this source extends between the components of the binary, to the south of the primary, but not north of the secondary (see §5.5).

All spectra have been shifted to the local standard of rest (LSR) velocity frame. Assuming a $V_{LSR} \sim 2$ km s^{-1} for the Cha I sources (James et al. 2006), we find that in all cases, the detected emission lines are centered at the rest wavelength of the $v = 1 \rightarrow 0$ $S(1)$ transition within the estimated measurement error ($\pm$ 1 km s^{-1}). In most cases, we find that the telluric correction was very effective, removing a significant number of telluric features. The remaining absorption lines are expected to be associated with the stellar photospheres of the target stars. As was found in previous detections of H_2 by Bary et al. (2002) and Bary et al. (2003), the H_2 features are resolved at this resolution. The FWHM for these lines fall within the range of $\sim 12 \leq v \leq 18$ km s^{-1} for the five TTS and slightly higher, ~ 20.4 km s^{-1} for the Herbig AeBe star. The H_2 equivalent widths and extinction corrected line fluxes are presented in Table 2 for the detections and one 'possible' detection (WW Cha whose spectrum is presented with the non-detections in Figure 1), along with the 3σ upper limits for the five sources that were clearly non-detections. The line fluxes were dereddened using A_v values from Gauvin & Strom (1992) and a standard $A_\lambda \sim \lambda^{-1.84}$ extinction law adopted from Martin & Whittet (1990).

In observations centered on the $v = 2 \rightarrow 1$ $S(1)$ rovibrational transition of H_2 at 2.2477 μm of two 2.1218 μm line emission sources, CS Cha and HD 97048, we did not detect line emission. The upper limits to the $v = 2 \rightarrow 1$ $S(1)$ line fluxes for CS Cha and HD 97048 are 6.5×10^{-16} and 4.4×10^{-15} ergs cm^{-2} s^{-1}, respectively.

4. DISCUSSION

The lack of bulk motion of emitting H_2 gas along the line of sight and with respect to the systemic velocity of the stars is interpreted as evidence that the gas is not entrained in a fast moving wind or outflow associated with any of these young sources. Additionally, the lack of extended emission beyond the full-width of the spectral beam indicates that the emitting gas is confined to regions within ~ 80 AU of the stars — with the exception of binary Glass Ia and Ib, in which the emission extends between the companions. Therefore, we conclude that, in all cases except Glass I, the emitting H_2 is quiescent gas residing in the circumstellar disks associated with these sources, and is not shocked, spatially extended gas, as has been observed toward other Class I sources and TTS (e.g., T Tauri, DG Tau; Herbst et al. (1996), Takami et al. (2004), Beck (2007)). The Glass I binary

TABLE 2
CHA I H_2 DETECTIONS AND NON-DETECTIONS

Source	K_{mag} [a]	Line Flux [b] (ergs cm^{-2} s^{-1})	Eq. Width (Å)	FWHM (km s^{-1})
Detections				
CS Cha	8.26	$2.1 \pm 0.1 \times 10^{-15}$	0.10	12.6
HD 97408	6.27	$8.6 \pm 0.4 \times 10^{-15}$	0.07	20.4
Sz 33	9.24	$6.9 \pm 0.3 \times 10^{-16}$	0.08	12.7
Glass Ia	8.58	$2.3 \pm 0.1 \times 10^{-15}$	0.43	12.1
Glass Ib	7.35	$6.7 \pm 0.3 \times 10^{-15}$	0.05	17.6
CV Cha	6.79	$2.0 \pm 0.2 \times 10^{-15}$	0.02	12.6
Possible Detection				
WW Cha	6.13	$\sim 3.7 \times 10^{-15}$	0.02	11.8
Non-Detections				
Sz 41	7.88	$<1.3 \times 10^{-15}$	···	···
LHα 332-17	6.26	$<3.0 \times 10^{-15}$	···	···
CHX 20E	9.19	$<3.9 \times 10^{-16}$	···	···
Sz 30	8.55	$<3.1 \times 10^{-15}$	···	···
HD97300	7.19	$<1.9 \times 10^{-15}$	···	···
Ced110 IRS 2	6.43	$<6.8 \times 10^{-15}$	···	···

[a] *K*-band magnitudes taken from Lawson et al. (1996) with the exception of Glass Ia and Ib found in Chelli et al. (1988).[b] The uncertainties in the line fluxes were determined based upon the continuum noise levels and the integrated line strengths.

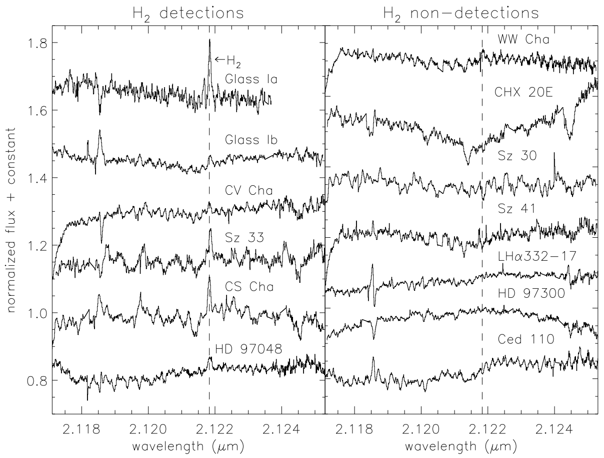

FIG. 1.— In the left frame, we plot the spectra for sources containing H_2 emission line features. The spectra have been telluric corrected and shifted into the V_{LSR} reference frame. We find that spectral features center on the rest wavelength of 2.1218 μm for the $v = 1 \rightarrow 0$ $S(1)$ transition of H_2 in the stellar rest frame, to within errors for the accepted V_{LSR} of Cha I members. In the right frame, we plot the spectra of the non-detections. These spectra have also been telluric corrected and shifted in the V_{LSR} reference frame of the sources. We note the inclusion of the spectra of WW Cha with the non-detections, but list it as a 'possible' detection in Table 2 due to the presence of a 2.4σ feature similarly centered at 2.1218 μm.

appears to be an exceptional source with its extended emission.

The small, but resolved FWHM measured for the quiescent emission features must be broadened by the Keplerian rotation of the gas as it orbits the central sources, since thermal broadening would require temperatures > 6000 K. Using the same technique Carr et al. (2001) and Najita et al. (2003) used to estimate the inner truncation radius of the gas disk using CO emission features, we used the velocity shift of H_2 gas at the outermost edges of the Gaussian-shaped features, referred to as the half-width at zero intenisty (HWZI), to estimate the innermost radius at which the detected H_2 gas resides. Assuming an inclination angle of 45°, the main sequence mass corresponding to the spectral type of each source, and estimating the maximum orbital velocity of gas from the HWZI, we calculated the inner radii for gas in the disks of CS Cha and Sz 33 to be 2.5 and 0.9 AU, respectively, while for the more massive stars, CV Cha and HD 97048, we find 3.2 and 5.5 AU. We note that these radii represent the innermost regions of the disks from which the emission arises and accounts for only a fraction of the overall line emission. We conclude that the bulk of the emitting gas resides outside of these disk radii.

The results we have found for the distances from the stars at which the hot H_2 emission is generated is similar to that found by Bary et al. (2003), who found FWHM of 9-14 km s^{-1} for several K type stars, placing the bulk of the emitting gas at about 10 AU, by Ramsay Howat & Greaves (2007), who found a line width of ~ 18 km s^{-1} for a single M3 star (ECHAJ0843.3-7905) and by Bitner et al. (2007), who found a line width of 8.5 km s^{-1} for a single AeBe star (AB Aur). In all of these cases, the H_2 gas emitting in rovibrational or pure rotational lines is not found close to the star (inside of 1 AU) nor at great distances from the stars, suggesting that processes exciting this emission is most effective at intermediate distances of a few to a few tens of AU from these stars.

Assuming that the emitting H_2 gas is optically thin, we have used Equation 2 from Bary et al. (2003), the measured line fluxes (see Table 2), and a distance of 160 pc to Chamaeleon I, to calculate the masses of 'hot' H_2 gas producing the line emission. We find that these masses fall within the range $10^{-11} - 10^{-10}$ $M_\odot$, in agreement with previous estimates (Bary et al. 2003; Ramsay Howat & Greaves 2007). On their own, these masses do little for informing us about the total mass of gas in the system or the total disk mass unless we understand the physical conditions of the gas and/or the mechanism responsible for stimulating the emission. We will address this problem in both §4.1 and §4.3.

4.1. $v = 2 \rightarrow 1$ $S(1)/v = 1 \rightarrow 0$ $S(1)$

The $v = 2 \rightarrow 1$ $S(1)/v = 1 \rightarrow 0$ $S(1)$ ratio has often been used to distinguish between two commonly observed mechanisms for stimulating H_2 emission: shock heating and UV fluorescence. The value of this ratio for a parcel of shock heated H_2 gas has been observed to be ~ 0.1, while a value of ~ 0.5 has been observed for UV fluorescent H_2 emission from low density gas ($n_H \leq 10^4$ cm^{-3}) (Black & van Dishoeck 1987; Gatley et al. 1987; Dinerstein et al. 1988). However, Burton et al. (1990) found UV fluorescent H_2 emission from clumpy photodissociation regions with shock-like values for the 2→1/1→0 line ratio and $n_H \geq 10^5$ cm^{-3}, suggesting that the value of 0.1 for the ratio is not unique for shock heated gas. In addition to these two processes, the response of H_2 gas irradiated by X-rays has been studied by several groups who conclude X-rays are capable of stimulating H_2 emission in a variety of astrophysical environments, including circumstellar disks (Gredel & Dalgarno 1995; Maloney et al. 1996;

Tine et al. 1997). Due to the collisional nature of the X-ray ionization process for stimulating H_2 emission, this mechanism also has been predicted to populate the excited rovibrational states of the H_2 molecules such that the $v = 2 \rightarrow 1$ $S(1)/v = 1 \rightarrow 0$ $S(1)$ ratio also has a value of ~ 0.1. Therefore, given the apparent degeneracy of the line ratio, differentiating between these three mechanisms will also require the knowledge of the density and kinematics of the emitting gas.

Nomura et al. (2007) present a detailed disk model that incorporates irradiation of the disk by X-rays and UV photons associated with the central source and includes dust grain growth and setting towards the midplane. Using this disk model, Nomura et al. (2007) calculate the level populations of H_2 in the model disk for a range of dust grain sizes and predict values for the $v = 2 \rightarrow 1$ $S(1)/v = 1 \rightarrow 0$ $S(1)$ H_2 line ratio for three stimulation scenarios: a) X-ray and UV, b) only UV, and c) only X-ray. The values Nomura et al. (2007) calculate for the line ratios differ significantly from the nominal values mentioned above and depend on sizes of the dust grains (see Figure 17 of Nomura et al. (2007)). They also find that as the dust grains grow and the grain opacity decreases, UV pumping should become the dominant stimulation mechanism over X-ray ionization. According to the findings of Nomura et al. (2007), an accurate measurement of the line ratio will determine the mechanism responsible for stimulating the H_2 emission as well as indicate the evolutionary status of the dust grain population.

The upper limits of the 2.2477 μm line observations mentioned in §3 can be used to determine an upper limit on the 2→1/1→0 line ratio for CS Cha and HD 97048. Unfortunately, with upper limits for the ratio of 0.4 and 0.5 for CS Cha and HD 97048, respectively, these observations lack the sensitivity in both cases to test the predictions of Nomura et al. (2007) and do not rule out the 'only UV' (scenario b) case.

Simultaneous observations of both lines made with a large aperture telescope and high resolution spectrometer (R $\geq$ 60,000) will be ideal for accurately measuring this line ratio. The simultaneity of these observations are important if the H_2 emission is variable, as non-simultaneous observations would then likely produce inaccurate measurements of the line ratio. Indeed, the H_2 emission is likely to be variable if the X-ray and UV fluxes, both known to be produced by highly variable phenomena in these young systems, are responsible for stimulating the H_2 molecules.

4.2. *Transitional Disks*

In the infrared, the shapes of the spectral energy distributions (SEDs) of cTTS systems are described as 'flat' due to emission from circumstellar dust grains in excess of the Rayleigh-Jeans tail of the blackbody curve observed for the stellar photospheres of main sequence stars. However, infrared photometric surveys of many TTS in nearby star forming regions, similar to those discussed in §1, also identified dips in the 1-10 μm regions of the otherwise flat SEDs associated with some of their targets (Strom et al. 1989; Skrutskie et al. 1990; Gauvin & Strom 1992). These findings suggest that the small warm dust grains responsible for the short wavelength infrared excesses in most cTTS disks are not present within the disks of these systems, while the cooler dust grains responsible for the longer wavelength excess persist in these disks. Therefore, the observed dips in the SEDs of TTS have been interpreted as evidence of holes or clearings in the innermost regions of these disks. These holes may arise due to the coagulation of small dust grains into planetesimals or the presence of a massive planet that dynamically cleared the inner regions of the disks (Skrutskie et al. 1990; Najita et al. 2007). Additionally, disk photoevaporation models, in which disk material is heated and 'boiled' away by highly energetic X-ray and UV photons, also have been offered as a phenomena responsible for the clearing of the inner holes in these transitional disks (Clarke et al. 2001; Alexander et al. 2006; McCabe et al. 2006).

For a few such transitional disk sources with inner holes extending out to several tens of AUs, such as GM Aur and CS Cha, tiny amounts of small dust grains, ~ 0.02 and 5×10^{-5} lunar masses, respectively, located within $\sim$1 AU, have been detected (Calvet et al. 2005; Espaillat et al. 2007). Somewhat surprisingly, several of these transitional disks possess well-known accretion signatures (i.e., $U-$band excess, strong H I recombination lines, etc.) suggesting that gas must remain within the disks and the inner holes, despite the lack of detectable dust emission. Chiang & Murray-Clay (2007) show that the accretion activity in these sources may be driven by coronal X-rays activating the magneto-rotational instability in the gas residing at the dust disk rim and residing within the inner disk hole.

4.2.1. *H_2 Emission from Transitional Disks*

All sources toward which we have searched for H_2 emission (Weintraub et al. 2000; Bary et al. 2002, 2003) known to possess transitional disks have been found to produce detectable levels of quiescent H_2 emission at 2.1218 μm, including TW Hya, LkCa 15, CS Cha, and GM Aur (Weintraub et al. (2005)); Bary et al. 2008, in prep). In each case, kinematic information from the emission lines, assuming a similar velocity dispersion as found for the other H_2 detections and for the unresolved feature measured for the disk of TW Hya[1] (Weintraub et al. 2000), places H_2 gas within the optically thin inner disk hole for each of these three sources. Rettig et al. (2004) detected $v = 1 \rightarrow 0$ rovibrational CO emission from the disk of TW Hya, but did not detect the $v = 2 \rightarrow 1$ CO band. Rettig et al. (2004) suggest that the absence of 'hot' CO gas indicates that the inner 0.5 AU of the disk has been cleared. A rotational temperature of $\sim$ 430 K leads these authors to conclude that the CO emission they detected in this system arises in warm gas occupying a very narrow annulus in the disk ranging between 0.5 and 1 AU. More recently, Salyk et al. (2007) detected warm CO emission from the disks of TW Hya and GM Aur, further confirming the presence of molecular gas in the inner regions of these transitional disks. Several of the other six sources detected in H_2 are classified as borderline c/wTTS or wTTS, including Sz 33 and DoAr 21 (Bary et al. 2002), which also makes them viable transitional disk candidates. Given that we estimate the innermost radius for the location of the gas producing the H_2 emission in these sources to be near ~ 1 AU, we conclude that these inner disk holes are not completely devoid of gas, in agreement with the detection and measurement of accretion activity in several sources possessing transitional disks.

---

[1] The detection of H_2 emission from TW Hya is reported as an unresolved detection in CSHELL spectra taken at the IRTF. The FWHM of the spectral feature was incorrectly quoted as < 6 km s^{-1} or the 1σ width. The FWHM of the unresolved line is actually measured to have a value of ~ 13.5 km s^{-1}, the instrumental resolution of the instrument.

We must consider whether this apparent correlation of H_2 emission with the presence of transitional disks could be the result of observational bias. Specifically, is H_2 emission easier to detect toward transitional disk sources because their near-infrared continuum flux levels are lower and thus do not overwhelm the H_2 line emission? If all cTTS generate some amount of quiescent H_2 emission, but sources with flat spectra and a resulting higher near-infrared continuum flux make detection of these narrow and weak spectral features more difficult, then the brightest K-band sources should be among the hardest toward which to detect quiescent H_2 emission. HD 97048, Glass Ib, and CV Cha, all of which are detected in H_2 emission, however, are among the brightest K-band sources in our sample. Therefore, we suggest that sources possessing transitional disks are preferentially detected in H_2 line emission because of physical conditions and phenomena intrinsic to these objects, rather than observational selection.

As discussed in §4.1, grain sizes have a notable effect on the cross-sections for UV and X-ray photons; consequently, as disks evolve and dust grains grow larger, the locations in a disk to which the photons penetrate and deposit their energies change (Nomura et al. 2007). As a result, the TTS that are sources of quiescent H_2 emission may be those that have disks that permit photons to penetrate to regions where the densities permit successful stimulation of H_2 emission. These disks would preferentially be those with optically thin inner regions and optically thick outer regions, i.e., transitional disk sources. For sources that are both X-ray and UV sources, a real dependence of the stimulation of quiescent H_2 emission on the size distribution of the dust grain population argues for UV fluorescence as the dominant stimulation mechanism, as UV cross-sections are much more dependent on the sizes of the dust grains.

4.3. *The H_2 Emitting Region*

In this section, we address the question of the location of the emitting H_2 gas stimulated by X-rays and/or UV photons, in the context of a transitional disk. We predict the regions of such disks in which the competing stimulation mechanisms will be most effective by finding areas of the disk bounded by optical depth surfaces associated with energetic photons. We then compare these regions with those determined from the kinematics of the emission features.

4.3.1. *UV & X-ray Optical Depth Surfaces*

Previous spectroscopic data (Bary et al. 2003) and those presented in this paper suggest that the emitting gas extends from ≥ 1 AU out to intermediate disk radii of 10-30 AU, with the bulk of the emitting gas residing at intermediate disk radii. We seek to determine if any agreement may exist between these empirically determined radii for the gas emission and those likely to be associated with emitting gas produced via the UV fluorescence and X-ray stimulation mechanisms.

Utilizing a standard TTS disk model (Glassgold et al. 1997), H_2 cross-sections found in Yan et al. (1998), and ignoring the contribution of dust and other trace gas components, to first order, we estimate where the UV photons and X-rays are absorbed and are likely to stimulate H_2 molecules in an atypical TTS disk devoid of small dust grains by calculating a range of optical depth surfaces for X-rays and UV photons with different energies impinging upon a disk with varying angles of incidence. The physical depth into the disk that each of these photons penetrates is determined by

$$\tau = \int_{r_{inner}}^{r_\tau} \kappa_\nu \left(\frac{\mathrm{r}}{\mathrm{r}_0}\right)^{-\mathrm{q}} \mathrm{dr}, \qquad (1)$$

where τ is the optical depth, r_{inner} is the radius at which the photons enter the disk, r_τ is the penetration depth of the photon for the given optical depth, $\mathrm{r}_0 = 1$ AU, q is the power-law index (here taken to have a value of 2.75), and κ_ν is the opacity of the H_2 for photons with frequency ν.The photons are assumed to enter the disk at 0.35 AU from the star, the innermost radius for which the model applies. After calculating the penetration depths (r_τ) for a range of energies and optical depths, plots of the optical depth surfaces were constructed (Figures 2 & 3) to illustrate the most likely regions of the disks in which the photons would be absorbed. The plots consist of density contours derived from the Glassgold et al. (1997) disk model overlaid with the optical depth surfaces. The thin black lines represent density contours derived from the disk model, while the bold black lines represent the optical depth surfaces. In Figure 2, we outline the surface corresponding to the uppermost boundary of penetration by either UV photons or X-rays (i.e., the $\tau = 1.0$ surface for a UV photon with energy 15.4 eV, corresponding to a wavelength of ~ 805 Å). This is the lowest energy for which the cross-section of an H_2 molecule can be determined using the models of Yan et al. (1998), and comes closest to matching the photon energies used in the UV fluorescence models of Black and van Dishoeck (1987).

In Figure 3, two optical depth surfaces are plotted with the upper bold contour representing for $\tau = 0.2$ for UV photons with the same energy as in Figure 2 and the second contour at lower disk elevation representing $\tau = 1.0$ for X-ray photons with an energy of 1 keV. Given the greater penetration depths associated with the X-rays, the $\tau = 1$ optical depth surface acts as the lower boundary for the penetration depth of the high energy photons. As illustrated by the plot, some of the X-rays are capable of penetrating into regions of the disk in which the densities exceed the critical density, ρ_c (where $\rho_c = 10^{-16}$ g cm^{-3} or 3×10^7 H_2 cm^{-3}; 4th model curve from the midplane) for the formation of the 2.1218 μm emission feature. Although some TTS are observed to produce X-rays with energies as high as 10 keV, we do not include them on this plot since they would penetrate to even greater depths and densities far exceeding ρ_c. We interpret the region lying between these two surfaces and above the critical density contour as location in the disk where the photons are most likely to deposit their energies and where the H_2 emission is most likely to originate. Using the constraints placed upon the location of the emitting region by the spectral information, we deduce that the bulk of the emission comes from a region located 10-30 AU from the star and 5-15 AU above the disk midplane.

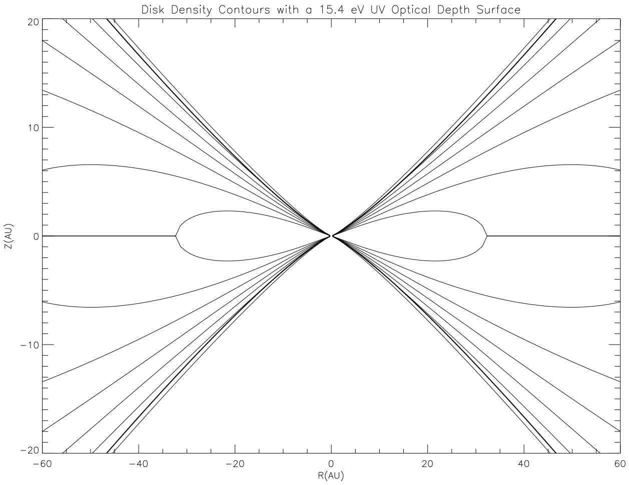

FIG. 2.— An optical depth surface ($\tau = 1$) for UV photons with an energy of 15.4 eV is plotted from 0.35 to $\sim$ 45 AU in bold black contours. The optical depth surface is overlaid atop density contours (thin contours) generated using the disk model of Glassgold et al. (2000). The density contour nearest the disk midplane represents a density of $\rho = 10^{-13}$ g cm^{-3}. With increasing elevation above the disk midplane, the values of the density contours decrease logarithmically, ending with $\rho = 10^{-19}$ g cm^{-3}. The optical depth surface roughly corresponds to the distance into the disk that photons with a wavelength of 805 Å could penetrate.

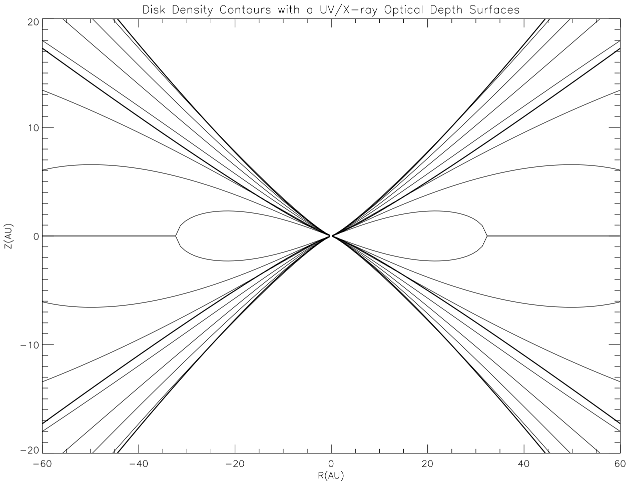

FIG. 3.— The $\tau = 0.2$ optical depth surface for 15.4 eV UV photons is plotted from 0.35 to $\sim$ 45 AU as a bold black line atop the disk density contours. The second bold black contour at lower disk elevation represents the $\tau = 1$ optical depth surface for 1 keV X-rays. The fourth curve from the midplane corresponds to 10^{-16} g cm^{-3} or 3×10^7 H_2 cm^{-3} which is the critical density for the $v = 1 \rightarrow 0$ $S(1)$ transition of H_2. It appears that most of the X-rays will penetrate to densities $n_{H_2} > 10^{-16}$ g cm^{-3}.

These calculations of optical depth surfaces demonstrate that the UV and X-ray photons most likely will deposit their energies in the upper levels of the disks at intermediate distances from the sources and confirm our earlier conclusions about the most likely location of the majority of the H_2 emission.

Having located the most likely region for the emitting H_2 gas, we next determine how much of the disk mass resides in the regions confined by the optical depth surfaces. By integrating the density profile of the disk model provided in Glassgold et al. (2000),

$$M_{disk} = \int_{r_{inner}}^{r_{outer}} \int_{0}^{2\pi} \int_{z_{lower}}^{z_{upper}} \rho_o \left(\frac{\mathrm{r}}{\mathrm{r}_0}\right)^{-\mathrm{q}} e^{\frac{-\mathrm{z}^2}{2\mathrm{H}^2}} \mathrm{rdrd}\phi\mathrm{dz}. \tag{2}$$

where r_{inner} and r_{outer} and z_{lower} and z_{upper} are the limits of integration for the radial and vertical extents of the portion of the disk to be considered, ρ_0 is the density of the disk at a radius of 1 AU and is equal to 1.4×10^{-9} g cm^{-3}, and H is the vertical scale height parameter given by $\mathrm{H}_0(\mathrm{r}/\mathrm{r}_0)^{1.25}$, where $\mathrm{H}_0 = 5 \times 10^{11}$ cm and $\mathrm{r}_0 = 1$ AU, we determine the mass of H_2 contained in the relevant regions outlined by the optical depth surfaces. Using Equation 2 and setting the inner (r_{inner}) and outer (r_{outer}) radial limits to 10 and 30 AU, respectively, and approximating the vertical limits, z_{lower} and z_{upper}, from the optical depth plots to be 5 and 10 AU, respectively, we find a mass of 2.8×10^{-5} $M_\odot$. This mass is more than enough to account for the observed emission. For comparison, only 5.8×10^{-9} $M_\odot$ lies in an upper region extending from $10 \leq \mathrm{z} \leq 15$ AU[2]. Since neither stimulation mechanism is 100% efficient, a mass larger than that contained in the horizontal layer from 10 to 15 AU should be expected to reside in the region of the disk where the emission originates. Therefore, the mass determined for the region 5 to 15 AU above the disk midplane suggests that the emitting gas likely extends downward, towards the midplane of the disk, with a minimum vertical height on the order of 5 AU at radii extending from a few to a few tens of AU for X-ray/UV stimulated H_2 emission in an accretionally-evolved disk associated with a TTS.

In our calculations of the optical surfaces for UV and X-ray photons, we have assumed that the gaseous component of the disk has been unaffected by the 'disappearance' of the micron-sized dust particles. If the gaseous component of the disk were to become more tenuous as the disk evolves, the resultant density structure would allow X-rays and UV photons to penetrate to even greater depths into the disk than suggested by the optical depth surfaces shown in Figures 2-6 and the critical density contour would move closer to the disk midplane and closer to the star. In this case, which is similar to that expected for a transitional disk, the emission could arise from gas in regions of the disk located much closer to the midplane and closer to the star, and from gas at even larger disk radii.

However, in the case of an evacuated inner disk, but a dust-filled outer disk, the opacities will increase in regions of the disk still populated by dust grains. Consequently, the shapes of the optical depth surfaces will change from those we have calculated. We note that

---

[2] Masses determined for the gas in the region of the midplane (0 AU) to 5 AU can be found in Table 3, but are not included in this discussion because the majority of this mass lies below the critical density contour, where no emission from the $v = 1 \rightarrow 0$ $S(1)$ can be produced.

TABLE 3
Masses in H_2 Source Regions

$r_{inner}\rightarrow r_{outer}$ (AU)	$z_{lower}\rightarrow z_{upper}$ (AU)	H_2 Mass ($M_\odot$)
10→30	0→5	6.4×10^{-3}
10→30	5→10	2.8×10^{-5}
10→30	10→15	5.8×10^{-9}

the extent of these inner holes is observed to vary from source to source and that these holes have observed sizes ranging from a few AU to ∼ 40 AU, suggesting slightly different conditions for determining the location of the emitting gas for individual sources.

Although the optical depth surfaces calculated in this section provide insight into the location of the emitting gas from an accretionally evolved disk, a calculation of these same surfaces employing the irradiated disk models of Nomura et al. (2007) and transitional disks, including a variety of cross-sections that incorporate the evolution of the size of dust grains will improve upon this investigation and make them applicable to a broad variety of accretionally-evolved circumstellar disks.

4.4. *H_2 & [Ne ii]*

The results of several investigations (Herczeg et al. 2007; Lahuis et al. 2007; Espaillat et al. 2007; Pascucci et al. 2006; Bary et al. 2008) have found four sources possessing [Ne ii] at 12.81 μm that also possess transitional disks. Of the four transitional sources possessing [Ne ii] emission, three (TW Hya, CS Cha, and GM Aur) also possess quiescent H_2 emission, while the fourth (DM Tau) has not yet been observed as part of any H_2 survey. The strong overlap between the transitional disk sources possessing both [Ne ii] and H_2 emission suggests a correlation exists between these two emission features and may be related to the nature of the transitional disks. In fact, because of the high initial ionization potential of 20.6 eV for [Ne ii] emission (Glassgold et al. 2007), this line probably traces the same high energy photons we theorize are responsible for stimulating the quiescent H_2 emission in the near-infrared. Furthermore, the FWHM measured for both the [Ne ii] and H_2 in TW Hya suggest that the emission from these two features arises at similar radii in the circumstellar disks.

5. INDIVIDUAL SOURCES

5.1. *CS Cha*

CS Cha was classified by Hartigan (1993) as a cTTS, based on a measured Hα EW of 65 Å, though Appenzeller et al. (1983; 13.3 Å) and Luhman (2004; 20 Å) found smaller values. The observed variability of Hα for CS Cha was previously suspected by Henize & Mendoza (1973). Gauvin & Strom (1992) and Persi et al. (2000), using IRAS and ISOCAM, respectively, found that CS Cha has little or no near-infrared excess but substantial mid- to far-infrared excesses. The magnitude and variability of the Hα EW measurements for CS Cha strongly suggest that this source is still actively accreting with a variable accretion rate — in support of this conclusion, Espaillat et al. (2007) estimated a mass accretion rate of 1.2×10^{-8} $M_\odot$ yr^{-1} for CS Cha from the *U*-band excess, while Johns-Krull et al. (2000) estimated it be 1.6×10^{-7} $M_\odot$ yr^{-1} — despite continuum measurements that the disk possesses an optically thin inner region.

Using *Spitzer* IRS spectra and MIPS photometry at 24 and 70 μm, Espaillat et al. (2007) modeled the SED for CS Cha and found a best-fit model that includes an inner hole with a radius of ∼ 43 AU, with a small amount of hot dust grains located between 0.1 and 1.0 AU. Based on the Espaillat disk model, the variable Hα measurements, the *U*-band excess, the strong [Ne ii] emission, and our detection of H_2 emission from the CS Cha disk, we suggest that CS Cha is an X-ray bright, actively accreting TTS possessing a transitional disk with a large optically thin inner hole, containing little dust and a significant amount of gas. The dust grain population is likely dominated by large grains, hence the low near-infrared excess, while the gas contributes substantially to the variable accretion rate.

5.2. *CV Cha*

LHα 332-21 is a binary cTTS (Reipurth & Zinnecker 1993), composed of CV Cha and CW Cha, having a large separation of 11.″7 (Ghez et al. 1997). We observed only CV Cha, the primary component, and have detected H_2 emission from this source. CV Cha has an Hα EW of 60.5 Å (Gauvin & Strom 1992) and exhibits weak continuum veiling in high resolution optical spectra obtained with UVES on the VLT (Stempels & Piskunov 2003). Extended UV emission has been detected in IUE observations of this source by Brooks et al. (2001). With a spectral type of G8V (Rydgren 1980; Takami et al. 2003) and a Log L_x of 30.1 ergs s^{-1} (Feigelson et al. 1993), CV Cha is one of most massive sources in our survey and one of the strongest X-ray emitters in the Chamaeleon I star forming region. This source is not known to possess a transitional disk and, due to a large Hα EW and the presence of the aforementioned continuum veiling, appears to be an actively accreting source. It appears that this source possesses the necessary attributes, in that it is a source of both UV and X-ray photons, to stimulate the observed quiescent H_2 emission.

5.3. *Sz 33*

Sz 33 has been classified as both a wTTS (Feigelson & Kriss 1989) and a cTTS (Feigelson & Lawson 2004) with a value of 9.5 Å for its Hα EW, placing it amongst the other transitional objects, "stradling" the line between a cTTS and wTTS (Gauvin & Strom 1992). Gómez & Persi (2002) present a low resolution (R ∼ 500) spectrum of Sz 33 that contains Paβ and Brγ emission features, indicating that this source is still actively accreting. Given the similarity of its ambiguous classification as a cTTS and/or a wTTS to other sources with detectable H_2 emission in our survey that possess optically thin inner disk regions, we suggest that the disk associated with Sz 33 also may be a transitional disk.

5.4. *HD 97048*

HD 97048 is classified as a B9.5V Herbig AeBe star, one of two Herbig AeBe stars that were observed as part of this survey (HD 97300 was the other). Our detection of quiescent near-infrared H_2 emission and the detection of pure rotational H_2 emission by Martin-Zaïdi et al. (2007) from this source places it in the company of AB Aur, another Herbig AeBe star, for which pure rotational H_2 emission has been detected by Bitner et al. (2007). Infrared emission from this source is thought to originate from the surface layer of a passively heated disk. Extended mid-infrared emission is dominated by a strong continuum produced by warm dust grains in the immediate vicinity of the star and solid state emission bands from silicates and carbonaceous materials (Meeus et al. 2001; Natta et al. 2001; Prusti et al. 1994). The spectrum rises rapidly longward of 2.2 μm and peaks around 60 μm (Hillenbrand et al. 1992; van Boekel et al. 2004) and is similar to the SEDs of TTS possessing transitional disks. An extended disk ranging from 360 to 720 AU was observed with the Advanced Camera for Surveys on the *Hubble Space Telescope.* Ca II, Na I, and O I are all observed in absorption suggesting that the source is neither actively accreting nor generating a bipolar outflow. Despite the absence of the accretion activity necessary for the production of UV photons in the low mass counterparts, copious amounts of UV radiation intrinsic to the SED of an early-type star as well as its detection as an X-ray source demonstrate the presence of the underlying mechanisms for high energy photon production we believe may be responsible for stimulating the H_2 emission.

5.5. *Glass Ia & Ib*

Glass Ia and Ib form a close binary system with a separation of $2''.4$, or a minimum physical separation of $\sim$ 380 AU. The secondary component is classified as an Infrared Companion (IRC) based upon the 2.2 μm flux ratio ($F_{2.2}$(optical primary)/$F_{2.2}$(IR companion)) (Natta et al. 2000) of 0.32. Hartigan (1993) and Natta et al. (2000) independently have categorized Glass Ia/Ib as a wTTS with a measured Hα EW of 4 Å. Lommen et al. (2007) did not detect 3.3 mm continuum emission from Glass I, suggesting that there are little to no mm-sized dust grains in the circumstellar and circumbinary environment.

The detection of H_2 emission from Glass I is quite unique amongst our other detections since it represents the only source for which we have detected spatially resolved emission. We have determined that all of the emission whether centered on the primary, the secondary, or in the extended emission, is centered on the stellar rest velocity with a dispersion of only 1.5 km s^{-1}, very near the estimated measurement error. Therefore, we find that the emitting H_2 gas in the system displays a common and systemic velocity.

When near-infrared H_2 emission is found to be spatially extended in the vicinity of a young star, the kinematics of the glowing gas typically reveal that it is associated with shocks in an outflow. The lack of dispersion in the central velocities of the extended H_2 emission features observed from the Glass Ia and Ib binary system, however, argue against the outflow scenario and indicate that this gas is associated with circumstellar and circumbinary disks in this binary system. Gas orbiting a 2 $M_\odot$ binary with a radius greater than 1700 AU will not produce a detectable velocity shift at this resolution. We do find that the FWHM of the emission features centered on both sources are slightly larger than those measured for the extended gas, with FWHM of 12.6 and 17.6 km s^{-1} found for the primary and the secondary, respectively, and 10.3 and 9.1 km s^{-1} measured for gas located $0''.8$ south the secondary and gas extending $0''.45$ to the south of the primary component, respectively. The difference in the FWHM measured for the components of the binary suggest that we are detecting emission from disks with different inclinations and/or central sources with different masses. For the extended gas, with its location likely to be in a circumbinary disk, little broadening of these lines will be contributed by the Keplerian motion. Assuming the standard thermal excitation temperatures for H_2 of 2000 K, the FWHM of the line is expected to be $\sim$ 7 km s^{-1}, slightly smaller than the FWHM measured for the extended emission features. The measured FWHM correspond to unreasonably high temperatures greater than 3000 K, perhaps, suggesting the presence of some turbulent broadening in the extended gas emission.

Although it is not currently possible to reconcile the broader than expected FWHM of the extended emission features with their origin in a circumbinary disk, it appears we can rule out the association of this emission with outflow activity. Since we find a larger FWHM for the lines centered on the components of the binary, and the FWHM is similar to those detected for the other detections in this survey, we infer that these features are associated with the circumstellar disks of the individual components.

5.6. *X-rays vs. Hα EWs*

In Figure 7, we present a plot of Log L_x versus Hα EW for all published H_2 detections and non-detections to determine if any correlation exists between these two parameters and the presence or absence of detectable quiescent H_2 emission. If H_2 emission is generated by X-rays produced in coronae and by accretion activity on the surfaces of these stars, we expect a clear correlation to exist between sources with detectable H_2 emission and their X-ray luminosities. Figure 7, however, shows that sources with a variety of X-ray fluxes, including a few sources without detectable X-ray fluxes, are among those with observed quiescent H_2 emission. Assuming that large intervening columns of circumstellar gas are not responsible for extinguishing the intrinsic X-ray luminosities of the apparently X-ray quiet sources, the lack of any correlation between H_2 detections and the presence and magnitude of a X-ray flux suggests that X-rays may not be responsible for stimulating the H_2 emission. On the other hand, there appears to be some correlation between Hα EW strengths and H_2 detections as all but a few sources in the region of the plot with Hα EWs greater than 10 Å (the rough boundary between cTTS and wTTS), produce detectable levels of H_2 emission. This correlation between Hα and H_2 emission links accretion activity with quiescent H_2 emission and are similar to the findings of Carmona et al. (2007). Since accretion activity in TTS is responsible for the production of the UV photons necessary to produce fluorescent H_2 emission, this correlation suggests that UV fluorescence is likely the dominant stimulation mechanism in some, if not all of the detections.

We now turn our attention to the transitional disk objects in Figure 7 denoted by the large asterisks overlaid upon the filled circles. Each of these sources (LkCa 15, CS Cha, and TW Hya) has been shown to possess an inner disk hole that is either devoid of dust grains or possesses an evolved population of large dust grains. In addition to these three transitional disk sources, HD 97048 has a similar infrared SED, as noted in §5.4, suggesting that it too possesses a large inner disk hole. If we consider that the other wTTS, Sz 33 and DoAr 21, are likely transitional disk objects, and, for the moment, ignore the binary sources GG Tau and Glass I due to their complexity, only three of the H_2 detections (CV Cha, ECHA J0843.3-7905, and LkHα 264) now appear as cTTS with non-transitional disks. However, the observations required to construct infrared SEDs do not currently exist in the literature. Future observations will be required to further test this correlation. Based upon the correlation we have found between transitional objects and quiescent H_2 emission, we conclude that objects detected in quiescent H_2 emission and designated as cTTS also may harbor transitional disks and that stimulation mechanisms responsible for producing the quiescent H_2 emission are likely related to both accretion activity and the evolutionary status of dust grains within their inner disks.

In addition to the possible impact of the evolutionary status of dust grains, the presence of UV and/or X-ray photons, and accretion activity on the production of quiescent H_2 emission, variability may also play a role in the detectability of these H_2 emission signatures. As in the case of most optical and infrared emission lines observed from TTS, the H_2 spectral features may fluctuate on similar timescales. We expect this variability to have a negative impact on our detection rate and may explain why some sources that share favorable characteristics with sources that are detections do not appear to produce detectable levels of H_2 emission. Therefore, variability may explain the lack of H_2 detections for some of the borderline cTTS seen in Figure 7. In order to determine if this is indeed the case, multi-epoch observations of some of the detections will be required to measure the magnitudes and timescales for any variability that may be associated with these sources. Simultaneous observations of the 2.1218 μm line as well as other accretion indicators also would be helpful in linking the emission with UV activity associated with accretion hot spots on the stars.

6. CONCLUSIONS

As part of a high resolution near-infrared spectroscopic survey for H_2 emission from TTS in nearby star forming regions, we have made new detections of emission features centered on the 2.1218 μm $v = 1 \rightarrow 0$ $S(1)$ transition of H_2 in the spectra of two cTTS (CS Cha and CV Cha), two wTTS (Glass Ia and Sz 33), one IRC (Glass Ib), and one Herbig AeBe star (HD 97048) located in the Chamaeleon I dark cloud. The detection of H_2 we report toward HD 97048 is the first detection of near-infrared emission from quiescent H_2 toward a Herbig AeBe star. In every case, the central velocity of the emitting gas is found to be coincident with the systemic velocity of the source. Assuming a circumstellar disk origin for these emission lines, an assumption well-supported by the central velocities of these lines falling at the rest velocities of the respective stars and by the narrow line widths, we used the HWZI and the FWHM velocities of these Gaussian-shaped emission features to estimate the innermost radii to which the gas extends and the radii at which the bulk of the emitting gas resides . We find that the innermost radii for all of the stars is on the order of $\sim$ 1 AU. We further find that the radii about which the bulk of the emission is centered is on the order of $\sim$ 10 AU. For the binary source (Glass I), H_2 emission extends between both components and to the south of the primary. Although the extended emission suggests that the gas could be entrained in an outflow, the lack of a detectable velocity gradient along the would-be axis of the outflow makes this an unlikely scenario. However, a circumbinary disk origin for the extended emission is also difficult to reconcile with the large FWHM of the emission lines measured for the extended emission.

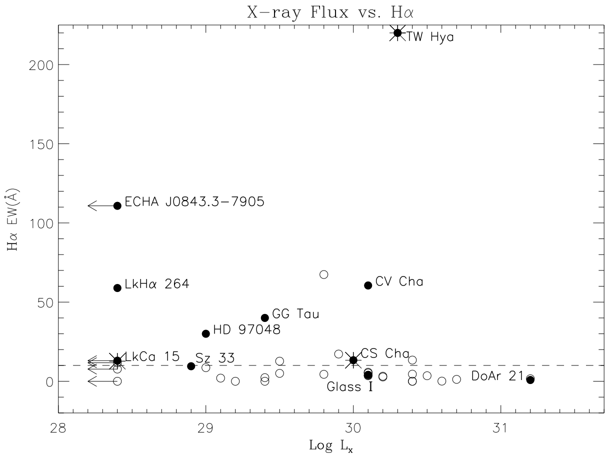

FIG. 4.— Log L_x versus Hα EW values for all sources with published observations of H_2 emission. The detections are denoted with filled circles and non-detections with open circles. Objects with known transitional disks are denoted by an asterisk. The horizontal dashed line designates the canonical dividing line at 10 Å separating cTTS (above) from wTTS (below). Arrows pointing to the left designate the sources which were non-detections in X-ray surveys. Detections are labeled with source names.

The initial goals for this survey was to determine if wTTS lacking detectable emission from standard disk tracers still harbor protoplanetary disks capable of or in the process of forming planetary systems. Our survey revealed two such stars, making a total of three, including DoAr 21 discovered by us in a previous survey.

The range of H_2 line fluxes ($6.9\times10^{-16} \leq F_{2.12} \leq 8.6\times10^{-15}$ ergs cm^{-2} s^{-1}) and masses ($10^{-10} \leq M_{H_2} \leq 10^{-11}$ $M_\odot$) measured for the Chamaeleon I sources with detected H_2 line emission were found to agree with all previous detections of quiescent H_2 emission. These trace amounts of gas do not directly inform us about the total disk masses harbored by these systems, though almost certainly the mass of H_2 detected directly through line emission at 2.1218 μm represents only a small fraction of the total mass in these disks. Our disk models suggest that the total disk masses could be 10^2 to 10^7 times greater than the mass measured directly in this single emission line.

Assuming that shock excitation is not the most likely mechanism for stimulating narrow line emission from H_2 gas which is not Doppler shifted from the systemic velocity of the source, we suggest that UV fluorescence and/or X-rays are the most likely stimulation mechanisms responsible for the observed H_2 emission. We calculated optical depth surfaces for UV photons and X-rays penetrating a disk composed entirely of H_2 to determine where in a core-accretionally evolved disk these photons deposit their energy and possibly generate H_2 emission. These models confirm that the radiation is most likely to be absorbed by gas in the upper atmospheres of these disks at intermediate radii and show that these stimulation mechanisms require significantly dense and massive columns of gas to produce the observed emission features at radii coincident with the those determined from the kinematic information. Many improvements may be made to these calculations by including opacities associated with large dust grains, other gaseous species, or a disk model that better approximates an irradiated transitional disk. However, the results from these calculations suggest that a gas-rich inner disk is necessary to produce quiescent H_2 emission via UV photons and X-rays, and that the stimulated gas resides at high disk altitudes and intermediate disk radii.

All four sources in our survey to-date known to possess transitional disks with optically thin inner disk holes are also H_2 detections. These detections place gas within the inner disk holes similar to the resolved and unresolved detections of [Ne II] emission lines from the sources. The presence of gas in the inner disk holes confirms the presence of gas within these gaps necessary to explain the accretion activity observed for these sources. The correlation between sources possessing quiescent H_2 emission and [Ne II] suggests a shared stimulation mechanism for both of these lines, a relationship to the photoevaporation process, and a distinct stage in the evolution of these circumstellar disks. We also find that most sources in our survey with Hα EWs sufficient to classify them as cTTS have detectable H_2 emission. The only exception is WW Cha, which may also be a detection, though we have cautiously classified it as a 'possible' detection, sine the H_2 emission towards this source, if real, is only at the 2.4σ level. The apparent relationship between Hα emission and accretion activity suggests that the quiescent H_2 emission may likewise be correlated with accretion in agreement with the findings of Carmona et al. (2007). This is not entirely surprising given that the UV photons necessary for stimulating H_2 emission are likely generated by accretion hot spots on the surfaces of the stars. In fact, this is strong evidence that UV fluorescence undoubtedly contributes to the observed H_2 emission. Given the dependence of the UV penetration depths on the sizes of the dust grains in the disk, illustrated by Nomura et al. (2007), and the overlap between H_2 detections and sources possessing transitional disks, we suggest that the evolutionary stage of the dust grain population in the inner regions of these disks is also correlated with the production of quiescent H_2 emission. Based upon these findings, we propose that Sz 33 and DoAr 21, both H_2 sources that are borderline c/wTTS, likely harbor transitional disks.

The authors would like to thank the staff members of Gemini South who were involved in collecting the data for this survey, especially Bernadette Rodgers, Phil Puxley, and Steve Ridgeway. The authors would also like to thank the anonymous referee for useful comments that improved the manuscript considerably. JSB acknowledges support from a NSF Astronomy and Astrophysics Postdoctoral Fellowship grant AST-0507310. JSB, DAW, JHK, and SJS acknowledge support from NASA Origins of Solar Systems (NAG5-13104) and from NSF AAG (AST-0307416).

REFERENCES

Alexander, R. D., Clarke, C. J., & Pringle, J. E. 2006, MNRAS, 369, 229

Appenzeller, I., Krautter, J., & Jankovics, I. 1983, A&AS, 53, 291

Bary, J. S., Weintraub, D. A., & Kastner, J. H. 2002, ApJ, 576, L73

—. 2003, ApJ, 586, 1136

Bary, J. S., Leisenring, J. M., & Skrutskie, M. F. 2008, in prep

Beck, T. L. 2007, AJ, 133, 1673

Beckwith, S. V. W., & Sargent, A. I. 1993, ApJ, 402, 280

Beckwith, S. V. W., Sargent, A. I., Chini, R. S., & Guesten, R. 1990, AJ, 99, 924

Bitner, M. A., Richter, M. J., Lacy, J. H., Greathouse, T. K., Jaffe, D. T., & Blake, G. A. 2007, ApJ, 661, L69

Black, J. H., & van Dishoeck, E. F. 1987, ApJ, 322, 412

Brooks, D. H., Costa, V. M., Lago, M. T. V. T., & Lanzafame, A. C. 2001, MNRAS, 327, 177

Burton, M. G., Hollenbach, D. J., & Tielens, A. G. G. M. 1990, ApJ, 365, 620

Calvet, N., D'Alessio, P., Watson, D. M., Franco-Hernández, R., Furlan, E., Green, J., Sutter, P. M., Forrest, W. J., Hartmann, L., Uchida, K. I., Keller, L. D., Sargent, B., Najita, J., Herter, T. L., Barry, D. J., & Hall, P. 2005, ApJ, 630, L185

Carmona, A., van den Ancker, M. E., Henning, T., Goto, M., Fedele, D., & Stecklum, B. 2007, ArXiv e-prints, 710

Carr, J. S., Mathieu, R. D., & Najita, J. R. 2001, ApJ, 551, 454

Chelli, A., Cruz-Gonzalez, I., Zinnecker, H., Carrasco, L., & Perrier, C. 1988, A&A, 207, 46

Chiang, E. I., & Murray-Clay, R. A. 2007, ArXiv e-prints, 706

Cieza, L., Padgett, D. L., Stapelfeldt, K. R., Augereau, J.-C., Harvey, P., Evans, N. J., II, Merin, B., Koerner, D., Sargent, A., van Dishoeck, E. F., Allen, L., Blake, G., Brooke, T., Chapman, N., Huard, T., Lai, S.-P., Mundy, L., Myers, P. C., Spiesman, W., & Wahhaj, Z. 2007, ArXiv e-prints, 706

Clarke, C. J., Gendrin, A., & Sotomayor, M. 2001, MNRAS, 328, 485

Damjanov, I., Jayawardhana, R., Scholz, A., Ahmic, M., Nguyen, D. C., Brandeker, A., & van Kerkwijk, M. H. 2007, ArXiv e-prints, 708

Dinerstein, H. L., Lester, D. F., Carr, J. S., & Harvey, P. M. 1988, ApJ, 327, L27

Espaillat, C., Calvet, N., D'Alessio, P., Bergin, E., Hartmann, L., Watson, D., Furlan, E., Najita, J., Forrest, W., McClure, M., Sargent, B., Bohac, C., & Harrold, S. T. 2007, ApJ, 664, L111

Feigelson, E. D., Casanova, S., Montmerle, T., & Guibert, J. 1993, Advances in Space Research, 13, 311

Feigelson, E. D., & Kriss, G. A. 1989, ApJ, 338, 262

Feigelson, E. D., & Lawson, W. A. 2004, ApJ, 614, 267

Feigelson, E. D., & Montmerle, T. 1999, ARA&A, 37, 363

Furlan, E., Hartmann, L., Calvet, N., D'Alessio, P., Franco-Hernández, R., Forrest, W. J., Watson, D. M., Uchida, K. I., Sargent, B., Green, J. D., Keller, L. D., & Herter, T. L. 2006, ApJS, 165, 568

Gatley, I., Hasegawa, T., Suzuki, H., Garden, R., Brand, P., Lightfoot, J., Glencross, W., Okuda, H., & Nagata, T. 1987, ApJ, 318, L73

Gauvin, L. S., & Strom, K. M. 1992, ApJ, 385, 217

Geers, V. C., Augereau, J.-C., Pontoppidan, K. M., Dullemond, C. P., Visser, R., Kessler-Silacci, J. E., Evans, II, N. J., van Dishoeck, E. F., Blake, G. A., Boogert, A. C. A., Brown, J. M., Lahuis, F., & Merín, B. 2006, A&A, 459, 545

Ghez, A. M., McCarthy, D. W., Patience, J. L., & Beck, T. L. 1997, ApJ, 481, 378

Glassgold, A. E., Feigelson, E. D., & Montmerle, T. 2000, Protostars and Planets IV, 429

Glassgold, A. E., Najita, J., & Igea, J. 1997, ApJ, 480, 344

Glassgold, A. E., Najita, J. R., & Igea, J. 2007, ApJ, 656, 515

Gómez, M., & Persi, P. 2002, A&A, 389, 494

Gredel, R., & Dalgarno, A. 1995, ApJ, 446, 852

Haisch, Jr., K. E., Lada, E. A., & Lada, C. J. 2000, AJ, 120, 1396

—. 2001, ApJ, 553, L153

Hamann, F., & Persson, S. E. 1992a, ApJS, 82, 247

—. 1992b, ApJS, 82, 285

Hartigan, P. 1993, AJ, 105, 1511

Henize, K. G., & Mendoza, E. E. 1973, ApJ, 180, 115

Herbst, T. M., Beckwith, S. V. W., Glindemann, A., Tacconi-Garman, L. E., Kroker, H., & Krabbe, A. 1996, AJ, 111, 2403

Herczeg, G. J., Najita, J., Hillenbrand, L. A., & Pascucci, I. 2007, ApJ, 670, 509

Herczeg, G. J., Wood, B. E., Linsky, J. L., Valenti, J. A., & Johns-Krull, C. M. 2004, ApJ, 607, 369

Hillenbrand, L. A., Strom, S. E., Vrba, F. J., & Keene, J. 1992, ApJ, 397, 613

Hinkle, K. H., Cuberly, R. W., Gaughan, N. A., Heynssens, J. B., Joyce, R. R., Ridgway, S. T., Schmitt, P., & Simmons, J. E. 1998, in Presented at the Society of Photo-Optical Instrumentation Engineers (SPIE) Conference, Vol. 3354, Proc. SPIE Vol. 3354, p. 810-821, Infrared Astronomical Instrumentation, Albert M. Fowler; Ed., ed. A. M. Fowler, 810–821

Hollenbach, D. J., Yorke, H. W., & Johnstone, D. 2000, Protostars and Planets IV, 401

Itoh, Y., Sugitani, K., Ogura, K., & Tamura, M. 2003, PASJ, 55, L77

James, D. J., Melo, C., Santos, N. C., & Bouvier, J. 2006, A&A, 446, 971

Johns-Krull, C. M., Valenti, J. A., & Linsky, J. L. 2000, ApJ, 539, 815

Kessler-Silacci, J., Augereau, J.-C., Dullemond, C. P., Geers, V., Lahuis, F., Evans, II, N. J., van Dishoeck, E. F., Blake, G. A., Boogert, A. C. A., Brown, J., Jørgensen, J. K., Knez, C., & Pontoppidan, K. M. 2006, ApJ, 639, 275

Lada, C. J., Muench, A. A., Haisch, Jr., K. E., Lada, E. A., Alves, J. F., Tollestrup, E. V., & Willner, S. P. 2000, AJ, 120, 3162

Lahuis, F., van Dishoeck, E. F., Blake, G. A., Evans, II, N. J., Kessler-Silacci, J. E., & Pontoppidan, K. M. 2007, ArXiv e-prints, 704

Lawson, W. A., Feigelson, E. D., & Huenemoerder, D. P. 1996, MNRAS, 280, 1071

Lommen, D., Wright, C. M., Maddison, S. T., Jørgensen, J. K., Bourke, T. L., van Dishoeck, E. F., Hughes, A., Wilner, D. J., Burton, M., & van Langevelde, H. J. 2007, A&A, 462, 211

Luhman, K. L. 2004, ApJ, 602, 816

Maloney, P. R., Hollenbach, D. J., & Tielens, A. G. G. M. 1996, ApJ, 466, 561

Martin, P. G., & Whittet, D. C. B. 1990, ApJ, 357, 113

Martin-Zaïdi, C., Lagage, P.-O., Pantin, E., & Habart, E. 2007, ApJ, 666, L117

McCabe, C., Ghez, A. M., Prato, L., Duchêne, G., Fisher, R. S., & Telesco, C. 2006, ApJ, 636, 932

Meeus, G., Waters, L. B. F. M., Bouwman, J., van den Ancker, M. E., Waelkens, C., & Malfait, K. 2001, A&A, 365, 476

Najita, J., Carr, J. S., & Mathieu, R. D. 2003, ApJ, 589, 931

Najita, J. R., Strom, S. E., & Muzerolle, J. 2007, MNRAS, 378, 369

Natta, A., Meyer, M. R., & Beckwith, S. V. W. 2000, ApJ, 534, 838

Natta, A., Prusti, T., Neri, R., Wooden, D., Grinin, V. P., & Mannings, V. 2001, A&A, 371, 186

Nomura, H., Aikawa, Y., Tsujimoto, M., Nakagawa, Y., & Millar, T. J. 2007, ApJ, 661, 334

Padgett, D. L., Cieza, L., Stapelfeldt, K. R., Evans, II, N. J., Koerner, D., Sargent, A., Fukagawa, M., van Dishoeck, E. F., Augereau, J.-C., Allen, L., Blake, G., Brooke, T., Chapman, N., Harvey, P., Porras, A., Lai, S.-P., Mundy, L., Myers, P. C., Spiesman, W., & Wahhaj, Z. 2006, ApJ, 645, 1283

Pascucci, I., Gorti, U., Hollenbach, D., Najita, J., Meyer, M. R., Carpenter, J. M., Hillenbrand, L. A., Herczeg, G. J., Padgett, D. L., Mamajek, E. E., Silverstone, M. D., Schlingman, W. M., Kim, J. S., Stobie, E. B., Bouwman, J., Wolf, S., Rodmann, J., Hines, D. C., Lunine, J., & Malhotra, R. 2006, ApJ, 651, 1177

Persi, P., Marenzi, A. R., Olofsson, G., Kaas, A. A., Nordh, L., Huldtgren, M., Abergel, A., André, P., Bontemps, S., Boulanger, F., Burggdorf, M., Casali, M. M., Cesarsky, C. J., Copet, E., Davies, J., Falgarone, E., Montmerle, T., Perault, M., Prusti, T., Puget, J. L., & Sibille, F. 2000, A&A, 357, 219

Prusti, T., Natta, A., & Palla, F. 1994, A&A, 292, 593

Ramsay Howat, S. K., & Greaves, J. S. 2007, ArXiv e-prints, 705

Ramsay-Howat, S. K., Harris, J. W., Gostick, D. C., Laidlaw, K., Kidd, N., Strachan, M., & Wilson, K. 2000, in Presented at the Society of Photo-Optical Instrumentation Engineers (SPIE) Conference, Vol. 4008, Proc. SPIE Vol. 4008, p. 1351-1360, Optical and IR Telescope Instrumentation and Detectors, Masanori Iye; Alan F. Moorwood; Eds., ed. M. Iye & A. F. Moorwood, 1351–1360

Reipurth, B., & Zinnecker, H. 1993, A&A, 278, 81

Rettig, T. W., Haywood, J., Simon, T., Brittain, S. D., & Gibb, E. 2004, ApJ, 616, L163

Rydgren, A. E. 1980, AJ, 85, 444

Salyk, C., Blake, G. A., Boogert, A. C. A., & Brown, J. M. 2007, ApJ, 655, L105

Sheret, I., Ramsay Howat, S. K., & Dent, W. R. F. 2003, MNRAS, 343, L65

Skrutskie, M. F., Dutkevitch, D., Strom, S. E., Edwards, S., Strom, K. M., & Shure, M. A. 1990, AJ, 99, 1187

Stempels, H. C., & Piskunov, N. 2003, A&A, 408, 693

Strom, K. M., Strom, S. E., Edwards, S., Cabrit, S., & Skrutskie, M. F. 1989, AJ, 97, 1451

Takami, M., Bailey, J., & Chrysostomou, A. 2003, A&A, 397, 675

Takami, M., Chrysostomou, A., Ray, T. P., Davis, C., Dent, W. R. F., Bailey, J., Tamura, M., & Terada, H. 2004, A&A, 416, 213

Tine, S., Lepp, S., Gredel, R., & Dalgarno, A. 1997, ApJ, 481, 282

van Boekel, R., Waters, L. B. F. M., Dominik, C., Dullemond, C. P., Tielens, A. G. G. M., & de Koter, A. 2004, A&A, 418, 177

Walter, F. M. 1992, AJ, 104, 758

Weintraub, D. A., Bary, J. S., Kastner, J. H., Shukla, S. J., & Chynoweth, K. 2005, in Protostars and Planets V, 8197–+

Weintraub, D. A., Kastner, J. H., & Bary, J. S. 2000, ApJ, 541, 767

Weintraub, D. A., Sandell, G., & Duncan, W. D. 1989, ApJ, 340, L69

White, R. J., & Basri, G. 2003, ApJ, 582, 1109

Yan, M., Sadeghpour, H. R., & Dalgarno, A. 1998, ApJ, 496, 1044

Zuckerman, B., Forveille, T., & Kastner, J. H. 1995, Nature, 373, 494